NANO LETTERS
Letter
Cite This: Nano Lett. 2018, 18, 6318−6325
pubs.acs.org/NanoLett

High-Precision Single-Molecule Characterization of the Folding of an HIV RNA Hairpin by Atomic Force Microscopy

Robert Walder,[†] William J. Van Patten,[†,‡] Dustin B. Ritchie,[∥] Rebecca K. Montange,[†] Ty W. Miller,[†] Michael T. Woodside,[∥] and Thomas T. Perkins*[,†,§]

[†]JILA, National Institute of Standards and Technology, and University of Colorado, Boulder, Colorado 80309, United States
[∥]Department of Physics, University of Alberta, Edmonton AB T6G 2E1, Canada
[§]Department of Molecular, Cellular, and Developmental Biology, University of Colorado, Boulder, Colorado 80309, United States

Supporting Information

ABSTRACT: The folding of RNA into a wide range of structures is essential for its diverse biological functions from enzymatic catalysis to ligand binding and gene regulation. The unfolding and refolding of individual RNA molecules can be probed by single-molecule force spectroscopy (SMFS), enabling detailed characterization of the conformational dynamics of the molecule as well as the free-energy landscape underlying folding. Historically, high-precision SMFS studies of RNA have been limited to custom-built optical traps. Although commercial atomic force microscopes (AFMs) are widely deployed and offer significant advantages in ease-of-use over custom-built optical traps, traditional AFM-based SMFS lacks the sensitivity and stability to characterize individual RNA molecules precisely. Here, we developed a high-precision SMFS assay to study RNA folding using a commercial AFM and applied it to characterize a small RNA hairpin from HIV that plays a key role in stimulating programmed ribosomal frameshifting. We achieved rapid data acquisition in a dynamic assay, unfolding and then refolding the same individual hairpin more than 1,100 times in 15 min. In comparison to measurements using optical traps, our AFM-based assay featured a stiffer force probe and a less compliant construct, providing a complementary measurement regime that dramatically accelerated equilibrium folding dynamics. Not only did kinetic analysis of equilibrium trajectories of the HIV RNA hairpin yield the traditional parameters used to characterize folding by SMFS (zero-force rate constants and distances to the transition state), but we also reconstructed the full 1D projection of the folding free-energy landscape comparable to state-of-the-art studies using dual-beam optical traps, a first for this RNA hairpin and AFM studies of nucleic acids in general. Looking forward, we anticipate that the ease-of-use of our high-precision assay implemented on a commercial AFM will accelerate studying folding of diverse nucleic acid structures.

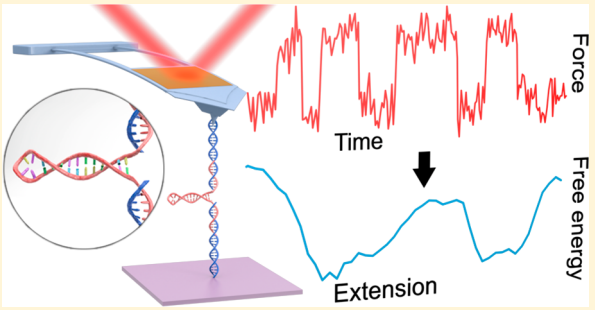

KEYWORDS: *Single-molecule force spectroscopy, RNA folding, kinetics, free-energy landscape, programmed ribosomal frameshifting*

Structured RNA molecules perform a wide range of vital functions within the cell. For example, ribozymes[1] and riboswitches[2] are intricately folded noncoding RNAs that respectively perform catalysis and regulate gene expression in response to ligand binding. Structures like pseudoknots and hairpin stem-loops can recode translation by stimulating deliberate shifts in the reading frame of the ribosome, thereby producing different proteins from the same mRNA sequence.[3,4] This diversity of functions arises from the specific folded configurations of the RNA. As a consequence, RNA folding has been the focus of decades of work using traditional biochemical and biophysical techniques.[1,2]

Starting in 2001, single-molecule force spectroscopy (SMFS) emerged as a powerful complementary tool for investigating the dynamics and energetics of RNA folding.[5] The pioneering SMFS studies of RNA folding used optical traps as the force probe,[5,6] and optical trapping has remained the dominant measurement platform.[7−14] Optical-trapping studies of diverse RNA molecules have revealed kinetic rate constants, energetics, intermediate states, folding pathways, and even a full 1D projection of the underlying free-energy landscape,[15,16] providing key insights into the connection between the biophysical properties of the RNAs and their biological function.[8,10−12,17,18] Critical to this scientific success is a potent combination of temporal resolution, force precision, and force stability that allows for both dynamic and equilibrium measurements. Moreover, individual molecules can be unfolded and refolded tens to hundreds or even thousands of times.

Received: June 26, 2018
Revised: September 19, 2018
Published: September 20, 2018

DOI: 10.1021/acs.nanolett.8b02597
Nano Lett. 2018, 18, 6318−6325

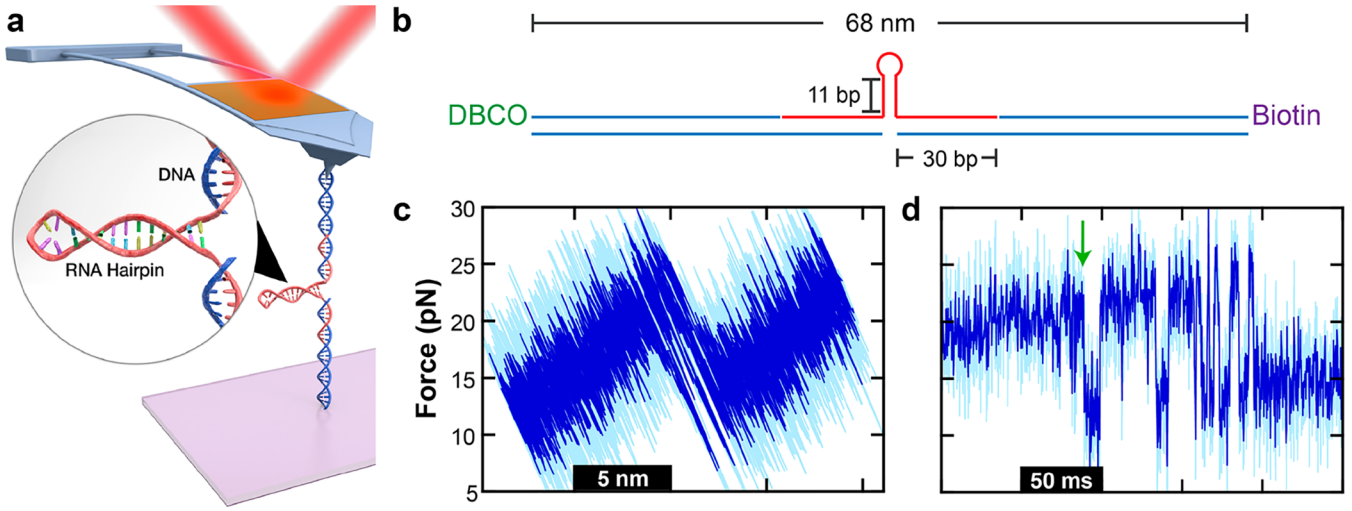

Figure 1. High-precision characterization of a small RNA hairpin from HIV that induces programmed ribosomal frameshifting. (a) Cartoon of the single-molecule force spectroscopy assay where a focused-ion-beam-modified cantilever applies force to an RNA hairpin via short double-stranded nucleic acid handles [RNA (red), DNA (blue)]. (b) Substrate schematic showing the hybrid RNA/DNA construct, which is covalently coupled at one end to an azide-functionalized, PEG-coated coverslip via dibenzocyclooctyne (DBCO) and attached reversibly at the other end to a streptavidin-coated AFM tip via biotin. (c) Force−extension curve showing the dynamics of the HIV RNA hairpin stretched at constant velocity (50 nm/s). Data were sampled at 50 kHz (light blue) and smoothed to 2 kHz (dark blue). (d) Force-vs-time trace from a brief segment of the data in (c) shows near-equilibrium fluctuations between the folded and unfolded states. The rupture force was determined from the first unfolding event (green arrow).

Unfortunately, this set of experimental capabilities typically requires custom-built instruments housed in specialized environments.[19] The construction, operation, and physical infrastructure needed for such advanced optical traps create significant barriers to the broader adoption of SMFS for characterizing RNA. In contrast, commercial atomic force microscopes (AFMs) are widely deployed and easy to use. AFM-based SMFS has had great success in studying mechanically robust proteins[20,21] and protein−ligand interactions[22,23] that rupture at high forces when retracting the cantilever at relatively rapid velocities (v = 50−5,000 nm/s). The challenges for AFM-based studies of RNA are the relatively poor force precision and stability of AFM in comparison to optical traps[24,25] in conjunction with the low forces at which RNA unfolding and refolding occur (typically in the range of ∼5−30 pN).[5,6] Indeed, studies of the same adenine riboswitch by AFM[26] and optical traps[18] show that AFM measurements have been unable to achieve the signal-to-noise levels present in a single optical-trapping record even when averaging dozens of measurements.

We overcame these challenges by developing a new high-precision assay for characterizing RNA folding on a commercial AFM and demonstrated its utility by studying a hairpin from HIV that induces programmed ribosomal frameshifting (Figure 1a). To do so, we integrated a series of recent technical advances in AFM-based SMFS[27−29] with a hybrid RNA/DNA construct (Figure 1b). Importantly, each end of the construct was site-specifically anchored,[30] a ubiquitous practice in other SMFS assays but still relatively rare in AFM-based ones.[24,25] When performing the standard dynamic assay where the cantilever is retracted at a constant velocity, we clearly resolved near-equilibrium unfolding and refolding transitions with high signal-to-noise ratio in individual records despite the rapid dynamics of this short hairpin (Figure 1c,d). By improving instrumental automation, we were able to unfold and refold an individual RNA molecule over 1,130 times. Enhanced force stability allowed us to measure folding dynamics at equilibrium that, in turn, enabled the reconstruction of the full 1D energy landscape for folding, the first such folding landscape reconstruction for a nucleic acid using AFM. Thus, by coupling our high-precision assay with the ease of use of a commercial AFM, we have developed a powerful yet accessible platform for characterizing the dynamics and energetics of diverse RNA molecules.

To demonstrate the capabilities of this platform, we studied a short hairpin from HIV that is of biological interest because it stimulates the ribosome to undergo a programmed −1 frameshift during the translation of the viral genome.[31−33] This hairpin provides a good test of our approach as it is quite small, consisting of an 11-base pair (bp) stem and 4-nucleotide (nt) loop, and is thus technically challenging to measure in comparison to 20 bp or longer hairpin structures often studied by SMFS using optical traps.[5,34] Moreover, this hairpin has been previously characterized at the single-molecule level,[9] including with a state-of-the-art dual-beam optical trap.[14] As a result, we have key reference data for assessing the performance of our AFM-based assay.

We first developed a single-molecule construct optimized for efficient measurement of diverse RNA molecules by AFM (Figure 1b). The overall concept is similar to constructs developed previously for optical-trapping-based studies: the target molecule is centered within double-stranded (ds) nucleic acid handles that link the molecule to the force probe while accommodating the geometric constraints of the assay.[5] Geometric constraints for high-precision optical trapping generally require constructs of 300−1,100 nm.[5,8] In contrast, we developed a short 68 nm construct consisting of two 70 bp dsDNA handles terminated with 30 nt segments of single-stranded (ss) DNA. The ssDNA segments in each handle were hybridized to complementary 30 nt sequences flanking the target RNA, providing a mechanically robust hybridization of the handles to the RNA. To anchor the construct covalently to the sample substrate, we used DBCO (dibenzocyclooctane), a copper-free click chemistry reagent, at

DOI: 10.1021/acs.nanolett.8b02597
Nano Lett. 2018, 18, 6318−6325

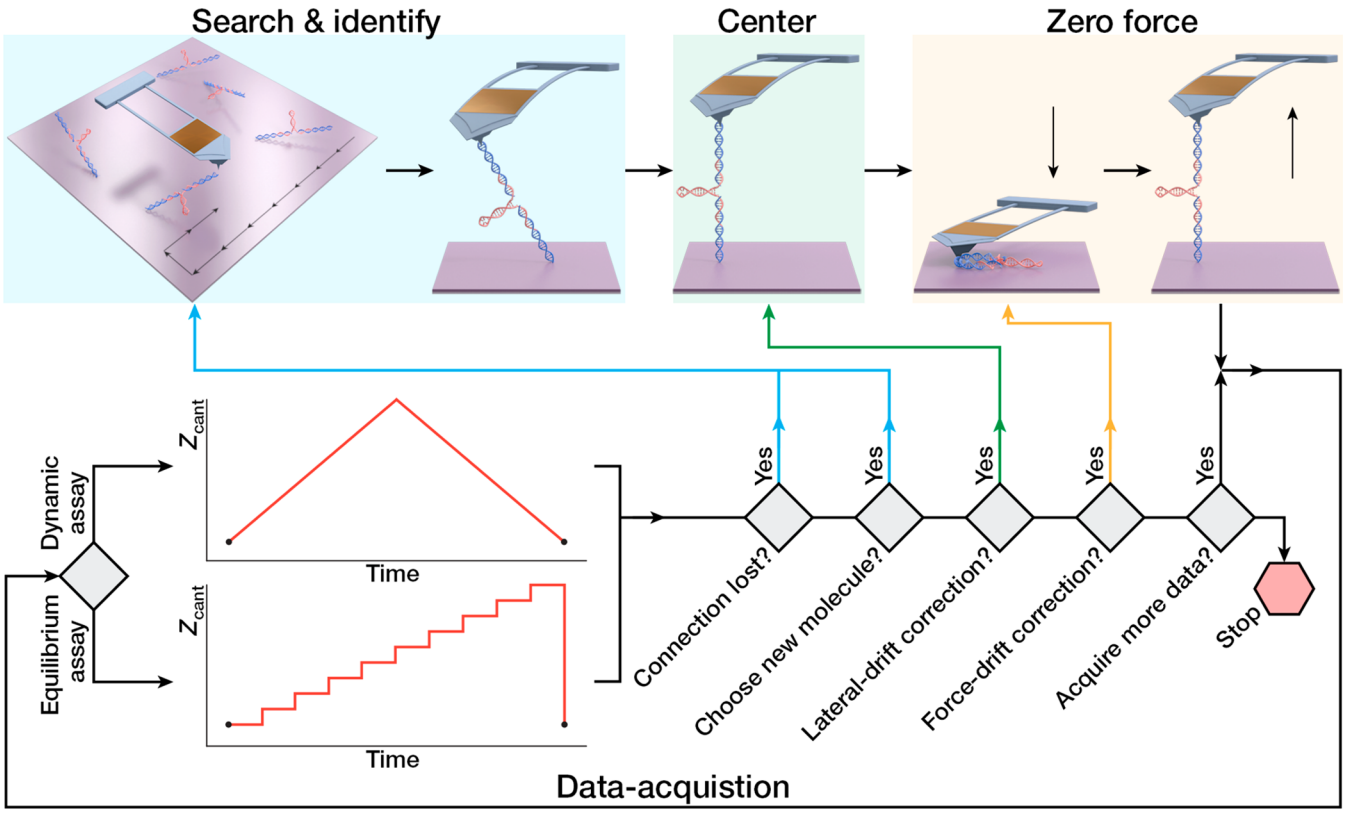

Figure 2. Flow diagram illustrating enhanced data-acquisition protocol. Each measurement starts with a trio of automated routines to search for and identify a candidate molecule, achieve a vertical pulling geometry by centering the assay, and determine the location of the surface and retract the cantilever until a specified extension is achieved. Both dynamic and equilibrium data can then be acquired. After each individual acquisition, the protocol checks for a series of conditions, such as loss of the connection. Other checks include looking for a new molecule, mitigating residual technical issues such as lateral stage drift (every 10 min) or force-drift correction (every 25−100 s), or simply acquiring more data. Typically, an automated data set for a single molecule involves unfolding and refolding the RNA molecule hundreds of times at several different velocities before acquiring a set of equilibrium trajectories at different extensions.

one end of one handle to attach to an azide-functionalized, PEG-coated coverslip.[30] We reversibly attached the other end of the construct, functionalized with biotin, to a PEG-coated AFM tip labeled with streptavidin.

To achieve state-of-the-art performance, we integrated several recent technical advances that improve the precision, stability, and accuracy of AFM-based SMFS.[27−29] We improved force precision and stability without sacrificing temporal resolution by reducing the stiffness and hydrodynamic drag of a commercial cantilever (BioLever Mini, Olympus) using a focused-ion beam (FIB).[28] We further improved force stability by removing the gold coating from the cantilever everywhere except for a small region near the free end of the cantilever (Figure 1a)[28] because the gold coating is the primary cause of force drift.[27] The resulting FIB-modified cantilevers featured a stiffness of ∼3−4 pN/nm, ∼40 μs resolution, and sub-pN force stability over 100 s (Figure S1). Finally, we achieved a 3-fold increase in force accuracy and precision by using a centering algorithm to align the attachment point of the construct to the AFM tip directly above the corresponding attachment point to the coverslip. This algorithm thereby achieved a vertical pulling geometry, avoiding pulling the construct at an angle, a significant issue for AFM constructs like ours with stiff polymeric handles (persistence length ≈ 50 nm).[29]

We complemented these improvements in the measurement of force with increased throughput by developing a significantly more sophisticated data-acquisition protocol (Figure 2). We initiated the assay in the standard manner, searching for a molecule by pressing the tip into the surface, albeit at a relatively low force (100 pN) to minimize surface adhesion. To detect a molecular attachment in real time, we next retracted the cantilever at a constant velocity (50 nm/s) and stopped the retraction if the force exceeded 20 pN at an extension of >30 nm, minimizing false triggering on tip−substrate adhesion. After running the centering algorithm,[29] the tip was then brought down into gentle contact with the surface to refine the measurement of the vertical surface position. After the completion of these initial steps, two measurement schemes were used: (1) to repeatedly measure unfolding and refolding events from an individual molecule in a dynamic assay, we moved the base of the cantilever (Z_{cant}) at a constant velocity to ramp the force up and down, sampling a range of different pulling speeds; (2) to measure unfolding and folding in an equilibrium assay, we held the base of the cantilever at a fixed position for 5 s while simultaneously measuring tip deflection as the molecule transitioned between folded and unfolded states. Importantly, these different data-acquisition schemes could be applied serially to the same individual molecule; other schemes, such as repeated jumping between a low and high force,[35,36] are in principle also compatible with this approach.

Using this data-acquisition protocol, we were routinely able to measure the folding of individual hairpins for 15−30 min

DOI: 10.1021/acs.nanolett.8b02597
Nano Lett. 2018, 18, 6318−6325

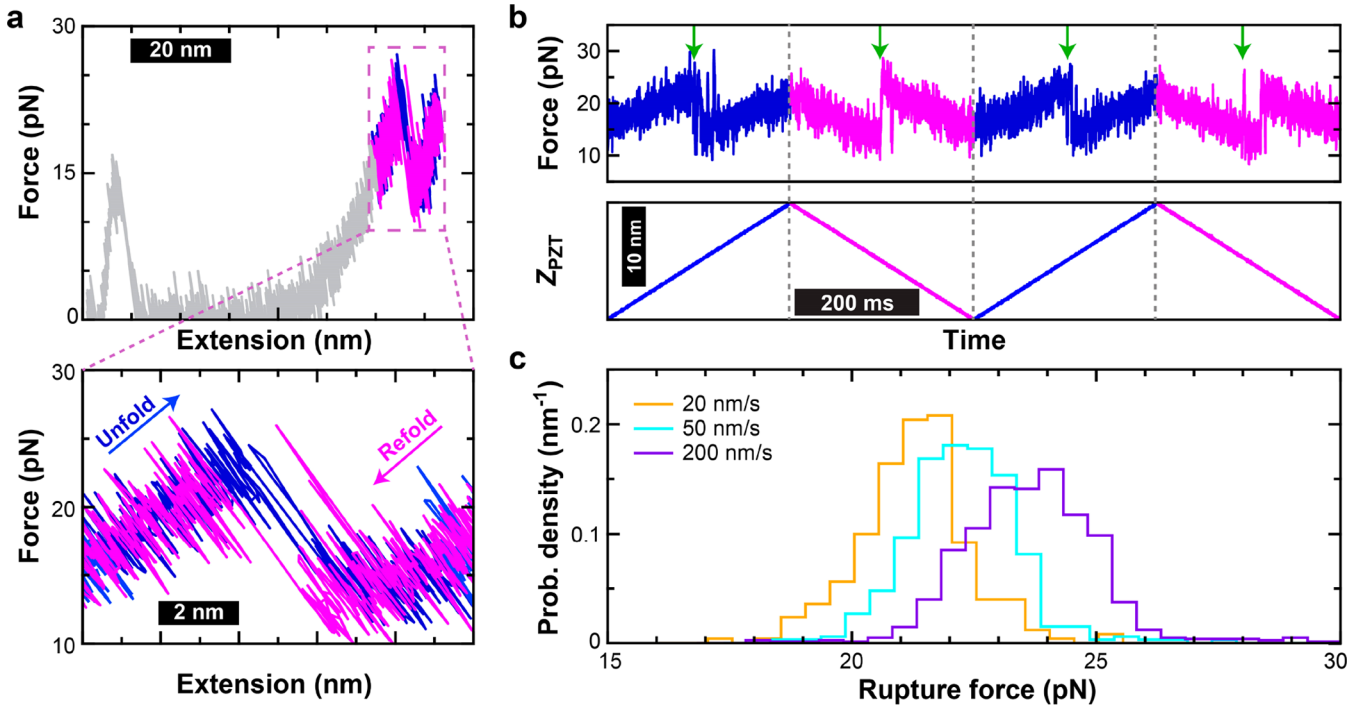

Figure 3. High-throughput characterization of an individual RNA hairpin in a dynamic force spectroscopy assay. (a) Force−extension curve showing the stretching of the RNA hairpin construct (gray) after running the zero-force routine. Next, the construct was alternately stretched (blue) and relaxed (magenta) by moving the cantilever at a given velocity (v = 50 nm/s) between fixed positions. For clarity, only one stretching-relaxation cycle is plotted (lower panel). A more detailed view of the force−extension curve shows near-equilibrium transitions occur while stretching and relaxing the construct. (b) Force-vs-time record (upper panel) showing repeated unfolding/refolding cycles driven by motion of the cantilever base (lower panel). The first unfolding or refolding event within each segment is denoted with a green arrow. (c) Probability distributions for the initial rupture force of the same individual molecule at pulling speeds of 20, 50, and 200 nm/s (N = 250, 332, and 800 rupture events, respectively). These pulling speeds correspond to mean loading rates of 21, 55, and 224 pN/s. Data shown in (a) and (b) were smoothed to 2 kHz.

with some molecules studied continuously for over 1 h. However, to do so, we needed to account for several ongoing technical limitations. First, there was still residual force drift [e.g., 0.5 pN over 100 s for a representative cantilever (Figure S1a)]. Although this level of drift is state-of-the-art by AFM standards,[24,25] the equilibrium distribution between the folded and unfolded states for a hairpin is sensitive to sub-pN changes in force.[5] To accommodate this high sensitivity to force, we repeatedly lowered the tip to gently touch the surface every ∼25−100 s, embedding a series of zero-force data points into the full record to facilitate computational subtraction of residual force drift. We also repeated the centering algorithm every ∼10 min to avoid changes in force associated with lateral stage drift. Ultimately, the duration of a single set of measurements on an individual molecule was limited by the noncovalent linkages in the assay. Because the tip was kept centered over the tether attachment point, we were often (although not always) able to reattach the molecule to the tip after rupture of either the streptavidin−biotin linkage or the 30 bp RNA/DNA hybridized segment.

To emphasize the utility of this integrated set of advancements, we rapidly acquired a dynamic force spectroscopy data set that contained several orders of magnitude more transitions than prior state-of-the-art for AFM-based studies of RNA folding.[26] For example, we characterized an individual hairpin at three different pulling speeds, acquiring 250, 332, and 800 unfolding and refolding curves at 20, 50, and 200 nm/s, respectively, over 15 min (Figure 3). After gently touching the surface to rezero the force, we stretched out the molecule to a preset extension (Figure 3a, gray). Next, the base of the cantilever was moved up and down at the desired velocity over a preset distance to unfold and refold the hairpin (Figure 3a, blue and magenta). This process was then repeated multiple times (Figure 3b) to obtain a distribution of initial rupture forces for that pulling velocity before repeating the whole procedure at different velocities (Figure 3c). Because of the fast dynamics of this short RNA hairpin coupled with the high temporal resolution of the FIB-modified cantilever (∼40 μs), we observed near-equilibrium transitions between the folded and unfolded states (Figure 1c,d; Figure 3a,b) at these low-to-moderate velocities. The histograms of initial rupture forces showed mean values and widths that increased with increasing pulling speed (Figure 3c) as expected[37,38] despite the relative low rupture forces of RNA hairpins in comparison to the traditional noise floor for AFM (∼5−20 pN).[24,25]

To complement this dynamic assay, we also demonstrated measurements of equilibrium folding and unfolding of an RNA molecule, a new regime for AFM-based studies of nucleic acids. For these measurements, the base of the cantilever was held fixed while recording the cantilever deflection for 5 s. By moving the position of the base of the cantilever in 2.5 Å steps, we shifted the distribution between the folded and unfolded state (Figure S2). As a result, we directly observed equilibrium hairpin dynamics when the folded and unfolded populations were approximately equal (Figure 4a). The unfolding/refolding dynamics of the hairpin were well resolved (Figure 4b) despite being very fast; analysis of the dwell times for the data in Figure 4a showed exponential distribution with an

DOI: 10.1021/acs.nanolett.8b02597
Nano Lett. 2018, 18, 6318−6325

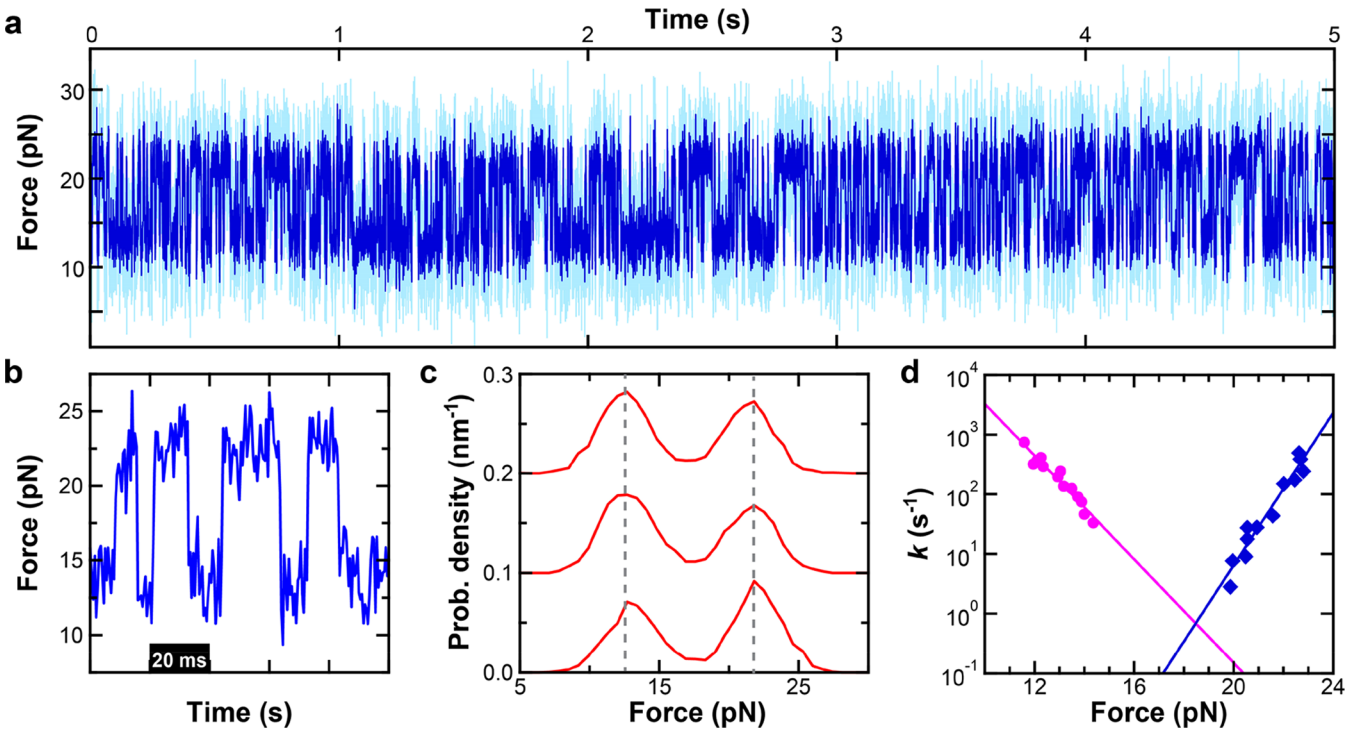

Figure 4. Equilibrium force spectroscopy of the HIV RNA hairpin. (a) Force-vs-time record showing rapid transitions between two states when the base of the cantilever was held at a constant position. Data were sampled at 50 kHz (light blue) and smoothed to 2 kHz (dark blue). A total of 710 transitions occurred in 5 s. (b) Folded and unfolded states well-resolved in a brief section of the record from (a). (c) Histograms from the first, second, and final third of the record from (a) showing the relative populations of the folded and unfolded states remain quite stable, indicating minimal force drift. (d) Force-dependent kinetic rate constants for folding (magenta) and unfolding (blue) determined from equilibrium measurements at different cantilever positions. Fitting the rates to the Bell model yielded the distance to transition state ($\Delta x^{\ddagger}$) and zero-force rate constant (k_0) for each state.

average lifetime of 7.0 and 6.3 ms for the unfolded and folded states, respectively (Figure S3).

Such equilibrium assays are technically challenging to implement because the ratio between the folded and unfolded state population can be extremely sensitive to small changes in the applied force. For instance, pioneering studies of RNA hairpins showed sensitivity to 0.1 pN changes in F around $F_{1/2}$ (the force at which the folded and unfolded states are equally populated).[5] To demonstrate the stability of our assay, we divided the trajectory shown in Figure 4a into thirds and computed histograms of the force to reveal any changes in the folded and unfolded state populations between each section of the record (Figure 4c). The consistency of the populations reflects our 0.15 pN force stability over 5 s, which is state-of-the-art for AFM studies[39] (Figure S1a).

Kinetic analysis of a set of such equilibrium trajectories is often used to determine two key parameters used to characterize folding: the zero-force rate constant (k_0) and the distance to the transition state ($\Delta x^{\ddagger}$). To do so, we determined the rate constant $k(F)$ for folding and unfolding at 12 different fixed positions of the cantilever base and therefore different forces (Figure 4d). Fitting to the Bell model,[40] $k(F) = k_0 \exp(\pm F\Delta x^{\ddagger}/k_BT)$ (where k_BT is the thermal energy, the positive exponent is for unfolding rates, and the negative exponent is for refolding rates), yielded $\log(k_0)$ [s^{-1}] = −12 ± 1, $\Delta x^{\ddagger}$ = 6 ± 2 nm for unfolding and $\log(k_0)$ [s^{-1}] = 8 ± 1, $\Delta x^{\ddagger}$ = 4 ± 1 nm for folding. Hence, this analysis indicates an asymmetric free-energy landscape with the transition state closer to the unfolded state consistent both with the general result for random hairpin sequences[34] as well as a prior optical-trapping study of this particular hairpin.[14]

Importantly, equilibrium assays enabled us to go beyond the limited characterization of the free-energy landscape offered by commonly used analyses like the Bell model to determine the full 1D free-energy landscape underlying folding. Such reconstruction was pioneered in optical-trapping studies of DNA hairpins,[34,41] but to date, it has only been realized in AFM work using high forces (~80−130 pN) in a recent study of membrane-protein dynamics.[42] In the present work, we analyzed the equilibrium trajectories of the HIV RNA hairpin using the inverse Boltzmann method.[34] This conceptually simple method makes use of the fact that, at equilibrium, the probability density at each extension, $p(x)$, is related to the free energy at that extension via $G(x) = -k_BT \ln[p(x)]$, as applied in early AFM studies of hydration layers.[43] In practice, the compliance of the handles and the cantilever broadens the measured probability density distribution, and this broadening needs to be removed via deconvolution, sharpening the distribution (Figure 5a, red vs blue).[34,44] Deconvolution requires an accurate measurement of this broadening, the point spread function. We measured the point-spread function for our assay using a reference construct consisting of the two handles bridged by a 60 nt DNA oligonucleotide, rather than the RNA hairpin, over the same range of forces used to characterize the hairpin while using the same particular cantilever (Figure S4). After deconvolution, the resulting free-energy landscape exhibited more confined potential wells and a higher barrier (Figure 5b). The barrier was asymmetric, and the position of the barrier top was consistent with the

DOI: 10.1021/acs.nanolett.8b02597
Nano Lett. 2018, 18, 6318−6325

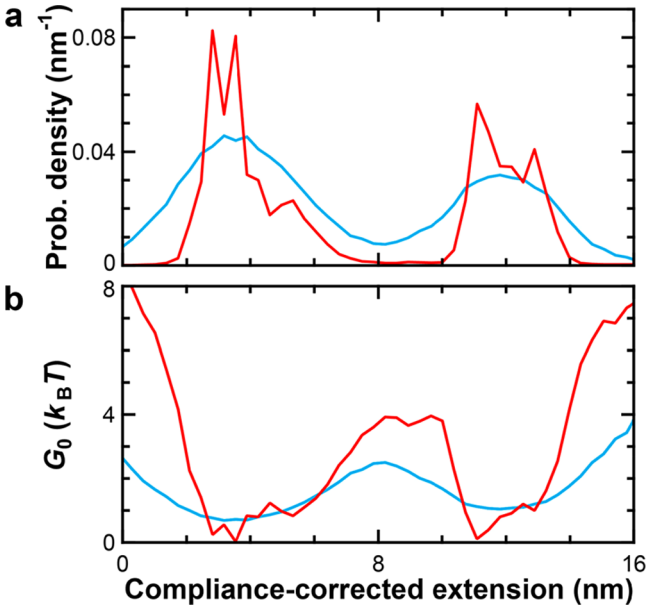

Figure 5. Free-energy landscape of the HIV RNA hairpin reconstructed using the inverse Boltzmann method. (a) Probability density of the compliance-corrected extension derived from the equilibrium trajectory shown in Figure 4a before and after deconvolving the effects of the handles and the cantilever (cyan and red, respectively). (b) Constant-force free-energy landscapes derived from the probability densities with and without deconvolution.

results of the above kinetic analysis. For clarity, the landscape is shown at a constant force (18.0 pN), where the minima of each of the two states are equal and the extension is corrected to account for the compliance of the handles and the cantilever.[45]

How do the SMFS results from our AFM-based study compare with previously reported ensemble- and optical-trapping-based studies? The primary point of comparison with ensemble measurements is the free-energy change between folded and unfolded states in the hairpin at zero force (ΔG_0). We calculated ΔG_0 from the single-molecule equilibrium trajectories based on the force-dependent occupancies of the folded and unfolded states, including a correction for the energy stored in the handles, cantilever, and unfolded RNA using a previously developed formalism.[46] The result, $\Delta G_0 = 29 \pm 1\ k_BT$, agreed reasonably well with the ensemble result of $25 \pm 1\ k_BT$ deduced from thermal melting using UV absorbance,[47] given ~10−15% uncertainty in the cantilever stiffness and hence the force and energy values.

Optical-trapping studies provided another basis for comparison because of the similarity of the measurements. The force at which unfolding and refolding rates were equal ($F_{1/2}$) (Figure 4d) was within the calibration error of the value found by optical trapping[14] (~18 vs ~16 pN). The location of the transition state was also consistent between AFM and optical trapping (6 ± 2 nm from the folded state vs 8.2 ± 0.8 nm) as was the zero-force unfolding rate ($10^{-9.9\pm0.7}$ vs $10^{-12\pm1}$ s^{-1}), notwithstanding the differences in the way the results were obtained: the AFM values were derived from an equilibrium assay whereas the optical-trapping ones were found from a dynamic one.

However, a noteworthy difference between optical-trapping and AFM equilibrium measurements was the rate at which the transitions occurred in equilibrium. Equilibrium AFM trajectories exhibited substantially faster kinetics due to the large change in force between the folded and unfolded states arising from the use of a much stiffer force probe and less compliant handles. Such acceleration of folding kinetics is beneficial because it increases the number of transitions that can be observed for a given measurement duration, helping to mitigate the detrimental effects of force drift. The degree of acceleration depends on the details of the system under study, but here, the force probe was ~10−20-fold stiffer and the DNA handles ~3-fold less compliant than prior optical-trapping studies of the same hairpin,[9,14] leading to ~100-fold more transitions per unit time than would occur in a constant-force optical-trap assay.[45] Put differently, in a constant-force assay with equal populations in each state, the rates of unfolding and refolding are necessarily the same. The extrapolation of the data in Figure 4c shows that this occurs at $F_{1/2}$ (18.2 pN), where the two lines intersect. The corresponding rates for each state is ~1 s^{-1}. In contrast, the data in Figure 4a shows the unfolded and folded states occurs at 12 and 22 pN, respectively, where the folding and unfolding rates are ~150 s^{-1}. The population in each state is the same, but the folded state unfolds more quickly than at constant force because it occurs at a force well above $F_{1/2}$. The same is true for the unfolded state, which occurs at a force below $F_{1/2}$. Hence, the unfolded state also folds more quickly relative to a constant-force assay. As a result, the force stability requirements for the AFM assay are relaxed compared to those for optical traps (i.e., the drift of 0.15 pN over a 5 s interval achieved here should be compared to the force stability of optical traps over a 500 s interval). To take advantage of this acceleration, however, one must use cantilevers with sufficient time resolution to resolve short-lived events. In this study, we used cantilevers with ~40 μs resolution, although other FIB-modified cantilevers offer resolution down to ~1−10 μs.[48,49] A potential disadvantage of the stiffness-induced acceleration of rates is that it may yield kinetics that are too fast for AFM to resolve, for example, in molecules that are close to the folding speed limit.[50]

In summary, we have developed an enhanced AFM-based SMFS assay for studying the folding of RNA and, more generally, nucleic acid structures. Combining high precision and temporal resolution with high force stability enabled the first AFM-based equilibrium measurements of a nucleic acid. From such trajectories, we derived not only the traditional SMFS parameters (k_0 and $\Delta x^{\ddagger}$) for a short hairpin from HIV but also the full 1D projection of the free-energy landscape. The improved quality and quantity of the data also enables incorporating additional advanced SMFS analyses.[51] For example, recent theory efficiently deduces $k(F)$ by analyzing near-equilibrium transitions between states.[52] Finally, the ease-of-use of our assay implemented on a commercial AFM circumvents the technical barriers involved in high-precision SMFS assays based on custom optical traps and thereby opens the door for a much broader range of applications and users.

■ ASSOCIATED CONTENT

Supporting Information

The Supporting Information is available free of charge on the ACS Publications website at DOI: 10.1021/acs.nanolett.8b02597.

DOI: 10.1021/acs.nanolett.8b02597
Nano Lett. 2018, 18, 6318−6325

Materials and methods, Figures S1−4, and Tables S1−S4, which contain oligonucleotide sequences (PDF)

AUTHOR INFORMATION

Corresponding Author

*E-mail: tperkins@jila.colorado.edu.

ORCID

Thomas T. Perkins: 0000-0003-4826-9490

Present Address

‡W.J.V.P.: Biophysics Graduate Group, University of California, Berkeley, California 94720, USA

Notes

The authors declare no competing financial interest.

ACKNOWLEDGMENTS

We thank Devin Edwards for fabricating FIB-modified cantilevers. This work was supported by the National Science Foundation (MCB-1716033; Phy-1734006) and NIST. Mention of commercial products is for information only; it does not imply NIST's recommendation or endorsement. T.T.P. is a staff member of NIST's Quantum Physics Division. M.T.W. acknowledges support from the John Simon Guggenheim Foundation.

REFERENCES

(1) Cech, T. R. Ribozymes, the first 20 years. *Biochem. Soc. Trans.* **2002**, *30*, 1162−1166.

(2) Serganov, A.; Nudler, E. A decade of riboswitches. *Cell* **2013**, *152*, 17−24.

(3) Brierley, I.; Dos Ramos, F. J. Programmed ribosomal frameshifting in HIV-1 and the SARS-CoV. *Virus Res.* **2006**, *119*, 29−42.

(4) Giedroc, D. P.; Cornish, P. V. Frameshifting RNA pseudoknots: structure and mechanism. *Virus Res.* **2009**, *139*, 193−208.

(5) Liphardt, J.; Onoa, B.; Smith, S. B.; Tinoco, I. J.; Bustamante, C. Reversible unfolding of single RNA molecules by mechanical force. *Science* **2001**, *292*, 733−737.

(6) Onoa, B.; Dumont, S.; Liphardt, J.; Smith, S. B.; Tinoco, I., Jr.; Bustamante, C. Identifying kinetic barriers to mechanical unfolding of the T. thermophila ribozyme. *Science* **2003**, *299*, 1892−1895.

(7) Liphardt, J.; Dumont, S.; Smith, S. B.; Tinoco, I., Jr.; Bustamante, C. Equilibrium information from nonequilibrium measurements in an experimental test of Jarzynski's equality. *Science* **2002**, *296*, 1832−1835.

(8) Greenleaf, W. J.; Frieda, K. L.; Foster, D. A.; Woodside, M. T.; Block, S. M. Direct observation of hierarchical folding in single riboswitch aptamers. *Science* **2008**, *319*, 630−633.

(9) Mazauric, M. H.; Seol, Y.; Yoshizawa, S.; Visscher, K.; Fourmy, D. Interaction of the HIV-1 frameshift signal with the ribosome. *Nucleic Acids Res.* **2009**, *37*, 7654−7664.

(10) White, K. H.; Orzechowski, M.; Fourmy, D.; Visscher, K. Mechanical unfolding of the beet western yellow virus −1 frameshift signal. *J. Am. Chem. Soc.* **2011**, *133*, 9775−9782.

(11) Frieda, K. L.; Block, S. M. Direct observation of cotranscriptional folding in an adenine riboswitch. *Science* **2012**, *338*, 397−400.

(12) Ritchie, D. B.; Foster, D. A.; Woodside, M. T. Programmed −1 frameshifting efficiency correlates with RNA pseudoknot conformational plasticity, not resistance to mechanical unfolding. *Proc. Natl. Acad. Sci. U. S. A.* **2012**, *109*, 16167−16172.

(13) Engel, M. C.; Ritchie, D. B.; Foster, D. A. N.; Beach, K. S. D.; Woodside, M. T. Reconstructing folding energy landscape profiles from nonequilibrium pulling curves with an inverse Weierstrass integral transform. *Phys. Rev. Lett.* **2014**, *113*, 238104.

(14) Ritchie, D. B.; Cappellano, T. R.; Tittle, C.; Rezajooei, N.; Rouleau, L.; Sikkema, W. K. A.; Woodside, M. T. Conformational dynamics of the frameshift stimulatory structure in HIV-1. *RNA* **2017**, *23*, 1376−1384.

(15) Tinoco, I., Jr.; Li, P. T.; Bustamante, C. Determination of thermodynamics and kinetics of RNA reactions by force. *Q. Rev. Biophys.* **2006**, *39*, 325−360.

(16) Savinov, A.; Perez, C. F.; Block, S. M. Single-molecule studies of riboswitch folding. *Biochim. Biophys. Acta, Gene Regul. Mech.* **2014**, *1839*, 1030−1045.

(17) Chen, G.; Chang, K. Y.; Chou, M. Y.; Bustamante, C.; Tinoco, I., Jr. Triplex structures in an RNA pseudoknot enhance mechanical stability and increase efficiency of −1 ribosomal frameshifting. *Proc. Natl. Acad. Sci. U. S. A.* **2009**, *106*, 12706−12711.

(18) Neupane, K.; Yu, H.; Foster, D. A.; Wang, F.; Woodside, M. T. Single-molecule force spectroscopy of the add adenine riboswitch relates folding to regulatory mechanism. *Nucleic Acids Res.* **2011**, *39*, 7677−7687.

(19) Neuman, K. C.; Block, S. M. Optical trapping. *Rev. Sci. Instrum.* **2004**, *75*, 2787−2809.

(20) Rief, M.; Gautel, M.; Oesterhelt, F.; Fernandez, J. M.; Gaub, H. E. Reversible unfolding of individual titin immunoglobulin domains by AFM. *Science* **1997**, *276*, 1109−1112.

(21) Puchner, E. M.; Gaub, H. E. Force and function: probing proteins with AFM-based force spectroscopy. *Curr. Opin. Struct. Biol.* **2009**, *19*, 605−614.

(22) Florin, E.-L.; Moy, V. T.; Gaub, H. E. Adhesion forces between individual ligand-receptor pairs. *Science* **1994**, *264*, 415−417.

(23) Hinterdorfer, P.; Dufrene, Y. F. Detection and localization of single molecular recognition events using atomic force microscopy. *Nat. Methods* **2006**, *3*, 347−355.

(24) Neuman, K. C.; Nagy, A. Single-molecule force spectroscopy: optical tweezers, magnetic tweezers and atomic force microscopy. *Nat. Methods* **2008**, *5*, 491−505.

(25) Greenleaf, W. J.; Woodside, M. T.; Block, S. M. High-resolution, single-molecule measurements of biomolecular motion. *Annu. Rev. Biophys. Biomol. Struct.* **2007**, *36*, 171−190.

(26) Heus, H. A.; Puchner, E. M.; van Vugt-Jonker, A. J.; Zimmermann, J. L.; Gaub, H. E. Atomic force microscope-based single-molecule force spectroscopy of RNA unfolding. *Anal. Biochem.* **2011**, *414*, 1−6.

(27) Churnside, A. B.; Sullan, R. M.; Nguyen, D. M.; Case, S. O.; Bull, M. S.; King, G. M.; Perkins, T. T. Routine and timely sub-picoNewton force stability and precision for biological applications of atomic force microscopy. *Nano Lett.* **2012**, *12*, 3557−3561.

(28) Bull, M. S.; Sullan, R. M.; Li, H.; Perkins, T. T. Improved single molecule force spectroscopy using micromachined cantilevers. *ACS Nano* **2014**, *8*, 4984−4995.

(29) Walder, R.; Van Patten, W. J.; Adhikari, A.; Perkins, T. T. Going Vertical to Improve Accuracy in AFM-Based Single-Molecule Force Spectroscopy. *ACS Nano* **2018**, *12*, 198−207.

(30) Walder, R.; LeBlanc, M.-A.; Van Patten, W. J.; Edwards, D. T.; Greenberg, J. A.; Adhikari, A.; Okoniewski, S. R.; Sullan, R. M. A.; Rabuka, D.; Sousa, M. C.; Perkins, T. T. Rapid characterization of a mechanically labile α-helical protein enabled by efficient site-specific bioconjugation. *J. Am. Chem. Soc.* **2017**, *139*, 9867−9875.

(31) Jacks, T.; Power, M. D.; Masiarz, F. R.; Luciw, P. A.; Barr, P. J.; Varmus, H. E. Characterization of ribosomal frameshifting in HIV-1 gag-pol expression. *Nature* **1988**, *331*, 280−283.

(32) Wilson, W.; Braddock, M.; Adams, S. E.; Rathjen, P. D.; Kingsman, S. M.; Kingsman, A. J. HIV expression strategies: ribosomal frameshifting is directed by a short sequence in both mammalian and yeast systems. *Cell* **1988**, *55*, 1159−1169.

(33) Bidou, L.; Stahl, G.; Grima, B.; Liu, H.; Cassan, M.; Rousset, J. P. In vivo HIV-1 frameshifting efficiency is directly related to the stability of the stem-loop stimulatory signal. *RNA* **1997**, *3*, 1153−1158.

(34) Woodside, M. T.; Anthony, P. C.; Behnke-Parks, W. M.; Larizadeh, K.; Herschlag, D.; Block, S. M. Direct measurement of the full, sequence-dependent folding landscape of a nucleic acid. *Science* **2006**, *314*, 1001−1004.

DOI: 10.1021/acs.nanolett.8b02597
Nano Lett. 2018, 18, 6318−6325

(35) Fernandez, J. M.; Li, H. Force-clamp spectroscopy monitors the folding trajectory of a single protein. *Science* **2004**, *303*, 1674−1678.
(36) Lannon, H.; Haghpanah, J. S.; Montclare, J. K.; Vanden-Eijnden, E.; Brujic, J. Force-clamp experiments reveal the free-energy profile and diffusion coefficient of the collapse of protein molecules. *Phys. Rev. Lett.* **2013**, *110*, 128301.
(37) Evans, E.; Ritchie, K. Strength of a weak bond connecting flexible polymer chains. *Biophys. J.* **1999**, *76*, 2439−2447.
(38) Dudko, O. K.; Hummer, G.; Szabo, A. Intrinsic rates and activation free energies from single-molecule pulling experiments. *Phys. Rev. Lett.* **2006**, *96*, 108101.
(39) Edwards, D. T.; Perkins, T. T. Optimizing force spectroscopy by modifying commercial cantilevers: improved stability, precision, and temporal resolution. *J. Struct. Biol.* **2017**, *197*, 13−25.
(40) Bell, G. I. Models for specific adhesion of cells to cells. *Science* **1978**, *200*, 618−627.
(41) Manuel, A. P.; Lambert, J.; Woodside, M. T. Reconstructing folding energy landscapes from splitting probability analysis of single-molecule trajectories. *Proc. Natl. Acad. Sci. U. S. A.* **2015**, *112*, 7183−7188.
(42) Yu, H.; Siewny, M. G. W.; Edwards, D. T.; Sanders, A. W.; Perkins, T. T. Hidden dynamics in the unfolding of individual bacteriorhodopsin proteins. *Science* **2017**, *355*, 945−950.
(43) Cleveland, J. P.; Schaffer, T. E.; Hansma, P. K. Probing oscillatory hydration potentials using thermal-mechanical noise in an atomic-force microscope. *Phys. Rev. B: Condens. Matter Mater. Phys.* **1995**, *52*, R8692−R8695.
(44) Gebhardt, J. C.; Bornschlogl, T.; Rief, M. Full distance-resolved folding energy landscape of one single protein molecule. *Proc. Natl. Acad. Sci. U. S. A.* **2010**, *107*, 2013−2018.
(45) Greenleaf, W. J.; Woodside, M. T.; Abbondanzieri, E. A.; Block, S. M. Passive all-optical force clamp for high-resolution laser trapping. *Phys. Rev. Lett.* **2005**, *95*, 208102.
(46) Stigler, J.; Ziegler, F.; Gieseke, A.; Gebhardt, J. C. M.; Rief, M. The complex folding network of single calmodulin molecules. *Science* **2011**, *334*, 512−516.
(47) Mouzakis, K. D.; Lang, A. L.; Vander Meulen, K. A.; Easterday, P. D.; Butcher, S. E. HIV-1 frameshift efficiency is primarily determined by the stability of base pairs positioned at the mRNA entrance channel of the ribosome. *Nucleic Acids Res.* **2013**, *41*, 1901−1913.
(48) Edwards, D. T.; Faulk, J. K.; LeBlanc, M. A.; Perkins, T. T. Force spectroscopy with 9-μs resolution and sub-pN stability by tailoring AFM cantilever geometry. *Biophys. J.* **2017**, *113*, 2595−2600.
(49) Edwards, D. T.; Faulk, J. K.; Sanders, A. W.; Bull, M. S.; Walder, R.; LeBlanc, M. A.; Sousa, M. C.; Perkins, T. T. Optimizing 1-μs-resolution single-molecule force spectroscopy on a commercial atomic force microscope. *Nano Lett.* **2015**, *15*, 7091−7098.
(50) Kubelka, J.; Hofrichter, J.; Eaton, W. A. The protein folding 'speed limit. *Curr. Opin. Struct. Biol.* **2004**, *14*, 76−88.
(51) Woodside, M. T.; Block, S. M. Reconstructing folding energy landscapes by single-molecule force spectroscopy. *Annu. Rev. Biophys.* **2014**, *43*, 19−39.
(52) Zhang, Y. J.; Dudko, O. K. A transformation for the mechanical fingerprints of complex biomolecular interactions. *Proc. Natl. Acad. Sci. U. S. A.* **2013**, *110*, 16432−16437.

DOI: 10.1021/acs.nanolett.8b02597
Nano Lett. 2018, 18, 6318−6325